Optimum conditions for preparative operation of capillary zone electrophoresis

A. Cifuentes, X. Xu, W.Th. Kok, H. Poppe*

*Amsterdam Institute for Molecular Studies (AIMS), Laboratory for Analytical Chemistry, University of Amsterdam,
Nieuwe Achtergracht 166, 1018 WV Amsterdam, Netherlands*

Abstract

The possibilities to use capillary zone electrophoresis (CZE) as a preparative tool have been studied, mostly from a theoretical point of view. The preparative performance of CZE is quantitated by the production rate, the amount of analyte that can be purified per unit of time. The production rate available with CZE is shown to depend in the first place on the chemical characteristics of the analyte–buffer combination. A figure of merit can be defined for a buffer system, describing its susceptibility to analyte overloading. Methods to find an optimal buffer system are referred to. It is shown that the loadability of the system is inversely proportional to the plate number required for the separation.

A second important factor for the maximum production rate is shown to be the thermal management of the instrumental system. The average increase of the solution temperature and the non-uniform migration velocity by temperature differences within the solutions are discussed. It is shown that in practical cases the temperature rise of the solutions will be the main limiting factor when high fields are used. With low fields, which in general give a higher production rate, siphoning of the solution becomes the dominant limitation for the production rate.

With cylindrical capillaries the highest production rate that can be obtained under practical conditions is in the order of $5 \cdot 10^{-13}$ mol s^{-1}. Experimental and theoretical results indicate that with rectangular capillaries the production rate can be increased by a factor of three.

1. Introduction

Capillary zone electrophoresis (CZE) is typically a miniaturized separation method. The paper by Jorgenson and Lukacs that set the whole technique off [1], clearly states the reasons for choosing a miniaturized system. The strong electric field one needs for obtaining a high speed of separation, in conjunction with the requirement to buffer both the pH and the conductivity of the carrier solution, inevitably leads to a large power dissipation per unit

volume. This can only be accommodated when the cross-sectional area of the electrophoretic duct is small, as otherwise the increase in temperature becomes too large. The common use of fused-silica as the tube material as well as the choice of inner diameters in the range of 10–100 μm are the practical consequence of this thermal management problem.

As indicated, strong electric fields are desirable; the length of the ducts is therefore commonly in the range 0.1 to 1 m. With the maximum total voltage drop being limited for practical reasons to a few tens kilovolt, separation times in the order of 10 min can be obtained.

* Corresponding author.

With these choices, the volume scale of the experiment is set: Typically, a 50 μm I.D. tube with a length of 0.5 m, and a volume (V_d) of approximately 1 μl is used, in which 100 000 theoretical plates (N) are generated. This leads to a volume standard deviation ($\sigma_{V,i}$) of the zone on elution of 3 nl. The sample concentrations one can use without undesired loss of resolution are limited by the so-called electromigration dispersion, EMD (this is maybe more properly indicated as concentration overload, but the term EMD is now quite generally used). When analyte concentrations are not small compared to the concentration of electrolytes in the buffer, both the pH and the conductivity in the zone will differ from that in the initial carrier liquid. This results in a dependence of migration rate on analyte concentration, distorting the symmetrical zones, eventually into triangular shaped peaks.

This upper concentration limit is rather low, for two reasons. In the first place a price has to be paid for the high efficiency so easily accessible in CZE. The above-mentioned 100 000 plates lead to a time standard deviation ($\sigma_{t,i}$) of solutes that equals 1/300 times the residence time (t_i) of a compound. It follows that a relative change in the migration rate of this order of magnitude already will be visible as peak distortion and loss of resolution in the electropherogram. Without further detailed considerations one may therefore assume, guessing that a 10% analyte–buffer concentration ratio would lead to 1% change in migration rate, that analyte concentrations must be not much larger than 1/30 of the carrier electrolyte concentration.

In the second place, the carrier concentration itself cannot be chosen very high, because of the above-mentioned thermal management problem. Thus, one hardly finds in contemporary literature carrier solutions more concentrated than 0.03 mol/l. Therefore, total amounts that can pass the CZE instrument without serious zone distortion, are in the order of

$$\sqrt{2\pi} \cdot \sigma_{V,i} \cdot c_{i,\mathrm{max}} = 2.5 \cdot 3 \text{ nl} \cdot 1/30 \cdot 0.03 \text{ mol/l}$$

$$= 8 \cdot 10^{-12} \text{ mol.}$$

The pico-, femto- and attomole detection limits reported for CZE have to be considered in this context. A picomole sensitivity is not so much of an effective advertisement for the technique when one realizes that this is also about the maximum the technique can effectively separate. That is, with picomole sensitivity peaks will either be distorted or suffer from a bad S/N ratio.

The analytical use of CZE is certainly hampered by this limitation, but the on-column detection, with simple UV absorption as well as with sophisticated electrochemical detectors and laser-based optical devices, has been improved to such an extent in the last ten years that many applications are possible with this miniaturized separation system.

The case of CZE forms an exquisite demonstration of the resolution–speed–capacity triangle once proposed by Scott and Kucera [2]. Without requirements on the capacity of the system one could have 40 kV across a 1-cm tube with 1 μm I.D., and separations in much less than a second.

2. Results and discussion

2.1. Production rate

Despite the miniaturized character of CZE, there is much interest [3–6] in the preparative operation of the technique, e.g., for the isolation of DNA fragments, drugs, peptides and proteins.

The production rate (T_i) can be defined as the amount of material i (in mol) that can be collected in purified form per time unit, averaged over a multiple of the separation time (or repetition time when regeneration of the system is required). This concept may appear slightly inappropriate in the present context, as it is associated strongly with preparative chromatography and technological 'unit operations' with an incomparably larger scale. Nevertheless, it is a useful concept as it applies to cases of repetitive operation as well as single separations. In the latter case T_i is just the ratio of amount collected and the run time. However, there might be cases where instrumental, physical or chemical con-

ditions would be such that repeated operation of a fast and small system would result in better productivity than one operation of a larger, slower system.

In analyzing the production rate we follow basically the same approach as has been used long ago by us in the case of preparative liquid chromatography (PLC) [7]. The mass flow, $f_i(t)$ (mol/s), at the exit of the system (index e) at time t is given by

$$f_i(t) = \tfrac{1}{4}\pi d_c^2 \cdot c_{e,i}(t) \cdot \mu_i E \qquad (1)$$

where d_c is the inner diameter of the capillary, $c_{e,i}$ is the concentration at the end of the capillary, μ_i is the electrophoretic mobility (with the electroosmotic mobility μ_{eo} included), and E is the strength of the electric field. The production rate T_i is found by averaging f_i over time. When $c_{max,i}$ is the maximum of $c_{e,i}$ and the peak is a Gaussian with a time standard deviation $\sigma_{t,i}$, the total amount collected in one run is equal to

$$\sqrt{2\pi} \cdot \tfrac{1}{4}\pi d_c^2 \cdot c_{max,i} \cdot \mu_i E \cdot \sigma_{t,i} \qquad (2)$$

and T_i is found after dividing by the run time. For the latter we take the residence time of the component in question, $t_{R,i}$, the difference being only in a numerical factor that depends on the particular mixture composition at hand, the set of mobilities and/or the time needed for regeneration of the system.

The same reasoning can be applied to other peak shapes, e.g., the triangular one that occurs when EMD determines peak broadening. One can even use the same Eq. 2, as the condition that the zones have a Gaussian shape, required to warrant the exact validity of Eq. 2, is not very strict. For other shapes one arrives at factors other than $\sqrt{2\pi}$ or 2.51, in Eq. 2. For those cases we define $\sigma_{t,i}$ as the square root of the centralized, normalized second time moment, e.g. the width/$\sqrt{12}$ for a block-shaped zone, or full width/$\sqrt{18}$ for a zone shaped as a rectangular triangle. For these two cases, simple algebra yields values of 3.46 and 2.12, respectively. As we are looking for general guidelines rather than precise quantitative relations, Eq. 2

is regarded as valid for all peak shapes of interest, including ones with triangular shape.

The result for T_i is:

$$T_i = \sqrt{2\pi} \cdot \tfrac{1}{4}\pi d_c^2 \cdot c_{max,i} \cdot \mu_i E \cdot \sigma_{t,i}/t_{R,i} \qquad (3)$$

which can also be written as:

$$T_i = \sqrt{2\pi} \cdot \tfrac{1}{4}\pi d_c^2 \cdot c_{max,i} \cdot \mu_i E \cdot N_{req}^{-1/2} \qquad (4)$$

The required plate number for the separation of the mixture at hand, N_{req}, is considered as a constant. Its value is determined by the relative mobilities of the components of interest and those possibly interfering with them. Eq. 4 shows that improving T_i amounts to increasing $c_{max,i}$, d_c (or the cross-section area A in cases where the electrophoretic duct is not cylindrical) and E. While doing so, however, the plate number should remain at least equal to the required plate number.

In the following it is assumed that the system is always operated at the maximum voltage available. Other parameters, such as the dimensions of the capillary and the type and concentration of the buffer (but not the pH, which is usually dictated by the nature of the sample mixture, and the selectivities required for good separation) can then be varied in order to obtain a maximum production rate.

Most of the equations used, often taken from literature, contain E as variable. As will be shown later, strong fields lead to small d_c values and small productivities; at weak fields the production rate is much higher, but the run times may become excessive. In view of the latter fact we found it more attractive from the practical point of view to take the run time (t_R) as the independent variable in graphs and tables. When the total voltage (ΔV) and t_R are known or assumed, the field strength and the capillary length can be calculated from:

$$L = (\mu_i \Delta V t_R)^{1/2} \qquad (5)$$

$$E = (\Delta V/(\mu_i t_R))^{1/2} \qquad (6)$$

However, in the equations these relations are usually not substituted, because that would lead to an unfamiliar form of many equations know from earlier work. Thus, all expressions con-

taining E and L should be interpreted with E and L given by Eqs. 5 and 6.

2.2. Chemical decisions

The electromigration dispersion, EMD, constant

Plate number, column diameter and field strength as occurring in Eq. 4 are strongly interrelated because of the thermal management problem discussed in a later section. The variable $c_{max,i}$, the maximum concentration of the target compound at the end of the duct, on the other hand, lends itself to straightforward discussion.

When resolution has to be preserved, the zone concentrations in CE must stay below a limit set by the EMD. The migration rate of a solute in its zone turns out to be dependent on the concentration, as a result of changes in conductivity (affecting the migration rate via changes in electric field) and, with protolyzing solutes, changes in pH, affecting the migration rate by changes in the effective mobility of the component.

The phenomenon, especially when caused by conductivity changes, has been investigated for non-protolyzing solutes and buffers by Mikkers et al. [8] and for weak acids and bases by Foret et al. [9]. The effect of pH changes has received little attention; recently, Beckers [10] applied a numerical procedure to obtain insight into this phenomenon. In our own work it has become possible to describe and predict this effect in two ways:

(a)   A numerical computer program [11], based on eigenvector description of the transport process, allows to predict the migration rate as a function of solute concentration, and to predict peak shapes. This approach applies to rather complicated electrophoretic systems, with solute and buffer components having up to five protolytic equilibrium stages, and up to four independent buffer constituents.

(b)   Recently [12], we found analytic solutions for the transport of monofunctional acids or bases in buffers based on monofunc-

tional acids or bases, taking into account the conductivity effect as well as the pH-shift effect.

Results of the two approaches are numerically the same. Together with the results cited above [8–12] they yield a common result of general importance. In this work we will restrict the discussion to cases of relatively small overload, such that extreme effects as, e.g., peak splitting, described and explained by Ermakov et al. [13], do not occur. If, moreover, the pH ranges between 3 and 11, the migration rate can be described with good accuracy, by the expression:

$$\mu_{app,i} = \mu_{eff,i}(1 + \beta_{EMD,i}c_i/c_b) \tag{7}$$

where c_b is some convenient measure for the concentration of the buffer mixture.

Before discussing this equation, a few notes on the nomenclature are in order. The index 'eff' refers to the averaging of mobilities over the various acid/base forms of the solute, at infinite dilution of the compound for the type and pH of the buffer used. The index 'app' refers to the migration rate of the zone. To obtain μ_{app}, the migration velocity is divided by the field *in the blank buffer*. This μ_{app} is not a genuine mobility, but it is a highly convenient variable to work with. The difference between μ_{app} and μ_{eff} reflects the change in electric field brought about by the change in conductivity within the zone, as well as the local change due to the pH shift, which is indeed a genuine change in mobility. We apologize in passing to those people who prefer to use the index 'app' for inclusion of the electroosmotic flow (EOF); we could not think of another convenient descriptive index. As the presence of EOF does not impair the reasoning in this paper as long as all mobilities are understood to include it, we decided to use this symbol.

The parameter $\beta_{EMD,i}$ is dimensionless. It describes the 'sensitivity' of the solute–buffer combination to electromigration dispersion. As an illustration we give one expression for a case where it can be derived easily for a 1:1 non-

protolyzing buffer (A^+, B^-) with a non-protolyzing solute (I^+). Then $\beta_{EMD,i}$ is given by:

$$\beta_{EMD,i} = \frac{(\mu_B - \mu_I)(\mu_A - \mu_I)}{(-\mu_A + \mu_B)\mu_I} \quad (8)$$

where the μ values are signed quantities. This is easily derived from the treatment presented by Mikkers et al. [8].

Another case where an explicit expression can be found, is that of a weak univalent acid or base as a solute in a buffer consisting of an univalent acid or base with an appropriate counter ion, as will be described in Ref. [12]. An important qualitative result from this work is that buffer conditions can be optimized to make $\beta_{EMD,i}$ approach zero, even if the mobilities do not match, by virtue of the cancelation of conductivity and pH-shift effects. Still, for the majority of practical solute–buffer combinations one has to resort to the numerical approach.

Peak shape under EMD conditions

The description of the triangular peak shape obtained under overload conditions is a long-standing result of the theoretical efforts in electrophoresis [8–10]. We shall therefore give only a brief account, just to put the derivations in our symbols.

Let us assume that the velocity of molecules i is described by:

$$u_i = u_{0,i} + \alpha c_i \quad (9)$$

an equation that seems equivalent to Eq. 7; the reasons for this re-formulation will become clear in the sequel.

The transport equation in CZE can be written as

$$\frac{dc_i}{dt} = -\frac{dJ_i}{dz} = \frac{-d(u_i \cdot c_i)}{dz} \quad (10)$$

where J_i is the mass flux of component i.

The migration rate of a point in the diffuse boundary with constant concentration, $u_{i,\text{diff}}$, i.e., the migration rate as we 'see' it, can be found by:

$$u_{i,\text{diff}} = \left(\frac{dz}{dt}\right)_{c_i} = -\frac{dc_i/dt}{dc_i/dz} = \frac{d(u_i c_i)/dz}{dc_i/dz}$$

$$= \frac{u_i \, dc_i/dz + c_i \, du_i/dc_i \cdot dc_i/dz}{dc_i/dz}$$

$$= u_i + \alpha c_i + \alpha c_i = u_{0,i} + 2\alpha c_i \quad (11)$$

The factor 2 in Eq. 11 reflects the difference between the species and boundary velocity. It seems that this point, well known since the work of Helfferich and Klein [14] for chromatography, has not been formulated explicitly in electrophoresis. Depending on the way the zone profile is derived, this can matter. A prediction of peak shape is usually and correctly [15] obtained by applying Eq. 9 directly to the *steep* boundary (where species velocity equals boundary velocity). The profile is then obtained by drawing a straight line between the point found and the one corresponding to $u_{i,0}$. This procedure is rather awkward and error-prone, since the maximum concentration usually varies on migration, and one thus has to integrate the velocity to obtain the travelled distance. Also, for long injection plugs that are still partially 'intact', this procedure becomes rather counter-intuitive. We prefer, as in earlier papers, to find the slope of the diffuse boundary directly, and this has to be done with Eq. 11. Note that the velocity of the steep boundary u_{shock} equals

$$u_{i,\text{shock}} = u_i + \alpha c_i \quad (12)$$

which makes clear why a rectangular injection plug eventually transforms into a rectangular triangle. With an α-value of the same sign as u_i, for instance the steep boundary at some point (in an infinite column) will be caught up by the faster moving diffuse boundary.

For triangular zones the position of the steep boundary is most easily found by applying the integral mass balance to find c_i; the area under the curve must match the injected amount. However, this discussion is not necessary in this paper.

It follows from all this that, indeed, Eq. 9 is not equivalent with Eq. 7. However, Eq. 11 is, with $\beta_{EMD,i} = 2\alpha/u_i \cdot c_b$. We will further work with Eq. 7, and not use Eqs. 9–12.

It is now possible to draw conclusions about the maximum c_i value admissible in (preparative) CE experiments. The plate number, N, originally a measure for real dispersion, is used here as an expression for the required sharpness of separation. It therefore prescribes also the maximum admissible 'electromigration dispersion'.

The zero-concentration end of the diffuse boundary is eluted at a time:

$$t_{R,i,0} = L/(\mu_{eff,i} \cdot E) \tag{13}$$

The peak maximum is eluted at a time:

$$t_{R,i,c} = L/(\mu_{eff,i}(1 + \beta_{EMD,i}c_{i,max}/c_b) \cdot E) \tag{14}$$

The difference is the peak width in terms of the full width of the triangle; it is to a high degree of accuracy equal to:

$$\Delta t_{R,i} = L/(\mu_{eff,i}E) \cdot (\beta_{EMD,i} \cdot c_{max,i}/c_b)$$
$$= t_{R,i} \cdot (\beta_{EMD,i} \cdot c_{max,i}/c_b) \tag{15}$$

A difficulty left is that the description of resolution is usually based on the assumption of Gaussian peaks, while the peaks here are triangular. As in the introduction, we (roughly) take as $\sigma_{EMD,i}$ the square root of the second moment. The factor between $\Delta t_{R,i}$ and $\sigma_{EMD,i}$ is, as stated before, $\sqrt{18} \approx 4.243$. Assuming (for the moment) that the freedom to allow peaks to be broad can be consumed entirely by the overloading, i.e. neglecting real dispersion, etc., one has:

$$\sigma_{EMD,i} = \frac{1}{4.243}\Delta t_{R,i} \tag{16}$$

$$t_{R,i}/\sigma_{EMD,i} = \sqrt{N_{req}} \tag{17}$$

leading to

$$c_{max,i} = 4.243/(\sqrt{N_{req}} \cdot \beta_{EMD,i}) \cdot c_b \tag{18}$$

Working via the second moment may provoke some doubts. Therefore, we also approach the matter more directly. It is generally recognized that resolution 4 (a distance of 4 standard deviations between the peak medians) gives acceptable separation. With two triangular peaks having the same sign and degree of shape deformation, Eq. 16 implies that with resolution 4, the

distance of the maxima is 4/4.243 times the full width of one zone. Thus, a few percent overlap occurs, as one would have with Gaussian zones with the same resolution. We therefore feel confident that the different shapes do not affect the validity of our conclusions.

Eq. 18, although not contradicting any intuitive guesses about the matter, is important as it allows some quite general conclusions:
1. The loadability in terms of concentration is directly proportional to the buffer concentration.
2. It is inversely proportional to the square root of the required plate number; the more difficult the separation, the smaller is the loadability.
3. Once one has determined the mobilities of the mixture components, and from that the required plate number, the loadability can be predicted 'ab initio', since with the methods described in the references mentioned, $\beta_{EMD,i}$ can be calculated.

The parameter $\beta_{EMD,i}$ allows to compare the usefulness of various buffer systems for separations where the compound i is critical: the smaller $\beta_{EMD,i}$ the better. Note that in $\beta_{EMD,i}$ the choice of the buffer concentration (by virtue of the 'relative' definition of it in Eq. 7), does not play a role. It is therefore necessary to discuss the choice of c_b separately.

Choice of buffer concentration c_b

In subsequent sections it will be discussed that often the product $d_c^2E^2\kappa$, where κ is the conductivity of the buffer solution, has to stay below an upper limit. In fact this product is a direct measure for the thermal dissipation in the lumen. Clearly, κ can be written as:

$$\kappa = \Lambda_b c_b \tag{19}$$

where Λ_b and c_b are the 'convenient measures' of the mean molar conductivity and concentration, respectively, of the buffer (in this paper, of the counter ion of the buffer).

The higher c_b, the higher $c_{max,i}$ can be, according to Eq. 18. However, high values for c_b preclude adjusting d_c and E to high values, when the product $d_c^2 E^2 \kappa_b$ should not increase above an upper limit.

Therefore, at a given value of the electric field E, the maximum value of κ, and as a result, the maximum values of c_b and $c_{max,i}$, are inversely proportional to d_c^2. Substituting this into Eq. 4 shows that *the production rate is unaffected by the choice of the buffer concentration*. What is gained in $c_{max,i}$ by higher buffer concentrations, is lost as a result of the smaller admissible d_c values. We note that Knox [16] reached quite another conclusion, which we believe is due to an incorrect assessment of the production rate.

Our conclusion holds, of course, only within reasonable limits. For instance, extremely high c_b values would require correspondingly high c_i values, which may be impossible due to limited solubility of a component i. Also, in very strong buffers the mobilities become unpredictable. On the other hand, extremely low c_b values would require large diameters for exploitation, which may be inaccessible due to gravity-induced convection and experimental limitations. Yet another exception occurs when siphoning effects become predominant (see below under 'Case III').

A final point is the influence of the conductivity, related to c_b via Eq. 19. The smaller the proportionality constant Λ_b the better, as this allows larger diameters at a given value for E. Thus the final 'figure of merit', $\Gamma_{b,i}$, for a buffer system for a solute i is not $\beta_{EMD,i}$ but rather its product with the mean molar conductivity, Λ_b:

$$\Gamma_{b,i} = \beta_{EMD,i} \cdot \Lambda_b. \tag{20}$$

As a example we provide in Table 1 data on the figure of merit of various buffer systems for the electrophoresis of a simple weak acid HZ with a pK_a of 4.7. It is supposed that the purification of HZ has to be carried out at a pH of 5. The buffers compared are of the anion–acid type (e.g. acetate–acetic acid), the cation–base type (e.g. ammonium–amine) and of the two basic–acid type, with different pK_a values.

The calculations show that an ideal buffer system of the anion–acid type exists in theory, giving no electromigration dispersion at all with a pK_a of approximately 4.5.

With a cation–base type of buffer there is always some electromigration dispersion; it can be minimized by choosing a buffer with a low pK_a value.

With the two basic–acid buffer the EMD is always relatively high; when this buffer is to be used a compound with a pK_a value of 5.3 gives the best results for this particular example. From Table 1 it is also clear that it is by no means straightforward to find the optimum buffer system for a cation.

2.3. Column design

Choice of d_c, L and E for cylindrical capillaries

As stated in the introduction, the conductive removal of the heat electrically generated in the lumen forms one of the limitations to the production rate. How large a temperature rise in the liquid can be tolerated, however, is not straightforward. One also has to distinguish between the elevation of the mean temperature on one hand and the thermal gradients in the lumen on the other hand.

The average temperature elevation may give rise to thermal decomposition of solutes, loss in efficiency due to enhanced longitudinal diffusion and badly reproducible results when the heat exchange is not constant. Radial gradients in the lumen may give rise to loss in efficiency as a result of non-uniform migration [17,18], in extreme cases also via gravity-induced convection. The mode of thermostatting and other experimental conditions determine which of the above effects will set the limit to the increase in d_c and E, desirable for improving the production rate. Treating all cases does not appear to be very useful. We will restrict the discussion to three cases, which in our opinion are the most appropriate, and broadly speaking, lead to the same conclusions. These are:

Case 1. The average temperature elevation ΔT_{max} is the limiting factor.

Table 1
Figure of merit Γ_b for the purification of a weak monobasic acid HZ

Type	Buffer pK_a	I_a counter ion (mol/l)	Λ_b $[\Omega^{-1}\,m^{-1}/(mol/l)]$	$\beta_{EMD,Aci}$	Γ_b $[\Omega^{-1}\,m^{-1}/(mol/l)]$
HA/A1−	3.9	0.0278	11.5	2.02	23.51
HA/A1−	4.1	0.0266	11.5	1.05	12.20
HA/A1−	4.3	0.0250	11.5	0.42	4.89
HA/A1−	4.5	0.0228	11.5	0.01	0.20
HA/A1−	4.7	0.0200	11.6	−0.24	−2.78
HA/A1−	4.9	0.0167	11.6	−0.40	−4.69
HA/A1−	5.1	0.0133	11.6	−0.50	−5.90
HA/A1−	5.3	0.0100	11.6	−0.57	−6.69
HA/A1−	5.5	0.0072	11.6	−0.61	−7.20
HA/A1−	5.7	0.0050	11.6	−0.64	−7.56
HA/A1−	5.9	0.0034	11.7	−0.67	−7.84
HA/A1−	6.1	0.0022	11.7	−0.68	−8.09
B/BH1+	3.9	0.0022	11.7	1.20	14.12
B/BH1+	4.1	0.0034	11.6	1.21	14.18
B/BH1+	4.3	0.0050	11.6	1.23	14.33
B/BH1+	4.5	0.0072	11.6	1.25	14.60
B/BH1+	4.7	0.0100	11.6	1.29	15.06
B/BH1+	4.9	0.0133	11.6	1.36	15.80
B/BH1+	5.1	0.0167	11.5	1.46	16.97
B/BH1+	5.3	0.0200	11.5	1.62	18.84
B/BH1+	5.5	0.0228	11.5	1.87	21.78
B/BH1+	5.7	0.0250	11.5	2.27	26.39
B/BH1+	5.9	0.0267	11.5	2.89	33.59
B/BH1+	6.1	0.0278	11.5	3.85	44.72
B/BH1+	6.3	0.0286	11.5	5.32	61.67
HA−/A2−	3.9	0.0855	13.9	−31.60	−439.59
HA−/A2−	4.1	0.0832	13.8	−17.49	−242.41
HA−/A2−	4.3	0.0799	13.7	−9.92	−136.75
HA−/A2−	4.5	0.0754	13.6	−5.70	−77.93
HA−/A2−	4.7	0.0697	13.5	−3.34	−45.28
HA−/A2−	4.9	0.0632	13.3	−2.09	−27.90
HA−/A2−	5.1	0.0562	13.0	−1.50	−19.66
HA−/A2−	5.3	0.0497	12.7	−1.33	−17.10
HA−/A2−	5.5	0.0441	12.5	−1.48	−18.64
HA−/A2−	5.7	0.0396	12.2	−1.96	−24.17
HA−/A2−	5.9	0.0364	12.0	−2.92	−35.31
HA−/A2−	6.1	0.0341	11.9	−4.74	−56.61
HA−/A2−	6.3	0.0326	11.8	−8.54	−100.98

Conditions: Solute HZ with a pK_a of 4.7 at a buffer pH of 5.0. Total buffer concentration 0.03 mol/l. Ionic mobilities (10^{-9} $m^2s^{-1}V^{-1}$) are: $\mu_{Z-} = -60$; $\mu_{A-} = -50$; $\mu_{BH+} = 50$; $\mu_{A2-} = -75$, $\mu_{counter-ion} = \pm 70$.

Case II. The non-uniformity plate height contribution is dominant.

Case III. The siphoning contribution to the plate height is dominant.

Case I. Average temperature elevation limited to ΔT_{max}, e.g., 10 K.

The average temperature elevation ΔT is in first-order approximation proportional to the

square of the tube diameter and to the power density:

$$\Delta T = r_{tot} \cdot d_c^2 \cdot \Lambda_b c_b E^2 \tag{21}$$

where the proportionality constant r_{tot} is the heat transfer resistance. As treated in some detail by Knox and Grant [18] and Grushka et al. [19], r_{tot} is built up of three main contributions, corresponding to the heat transfer resistance of the lumen, the wall and the surrounding thermostatting medium:

$$r_{tot} = r_{lum} + r_{wall} + r_{thm} \tag{22}$$

As shown by many workers [16,17,19], r_{lum} and r_{wall} can be easily predicted:

$$r_{lum} = 1/(16k_s) \tag{23}$$

$$r_{wall} = 1/(8k_{wall}) \cdot \ln(d_o/d_c) \tag{24}$$

Here k_s and k_{wall} are the thermal conductivities of the solution and wall, respectively, and d_o is the outer diameter of the tube.

Unfortunately, r_{thm}, which is by far the largest contribution in practice (see e.g., discussion by Ermakov and Righetti [20]), cannot be calculated easily. It depends on the diameter of the tube, and in a complicated fashion on the flow regime and the properties of the thermostatting fluid. It is therefore probably better to approach the matter from the experimental point of view. Since ΔT-values are experimentally easily accessible via the voltage–current ratio, there are various sources of data on this point.

Bruin et al. [21] found an experimental value of $r_{thm} = 4.2$, using air thermostatting and capillaries of 50 μm I.D. and 335 μm O.D., while Nielsen et al. [22] found a value of $r_{thm} = 4.1$ with forced air convection and capillaries of 75 μm I.D. and 360 μm O.D.

Standard texts on heat transfer [23,24], as well as the discussions by Knox et al. [16,25], make clear that a constant value for r_{thm} (i.e. a constant Nusselt number [24–26]) is very unlikely. It could only occur when heat transport by pure conduction in the thermostatting fluid takes place over a distance having a fixed proportion to the tube diameter. The fluid moves either because of the thermostatting fan or by natural,

gravity-induced convection. The larger the diameter and/or the fluid velocity, the more heat is transported by convection and the smaller will be the r_{thm} values.

Although there are useful treatments of these effects available in chemical engineering science, these are not used in this paper. The reason is that we believe that the thermal conditions of a CE capillary are much too complicated to make such a treatment useful. The most important point here is the longitudinal non-uniformity. Two parts of the tubes (in the buffer vials) are in fact liquid-thermostatted, three parts at least (in both vials and in the detector) are in stagnant air and the remainder is in an air or liquid bath with a flow being non-uniform in intensity and direction across the tube length. In some instruments even half of the capillary may not be under proper thermostatting. Longitudinal gradients, likely in all CE equipment with liquid- or air-thermostatting, affect the electroosmotic flow, thereby inducing parabolic components in the velocity and giving rise to additional non-uniformity dispersion [27,28].

We shall work in the sequel with a constant value of 5.0 K/(W/m) for r_{tot}, a rough average of experimental values.

Eq. 22 can be then solved for the maximum d_c allowed when temperature increase is limiting:

$$d_c^2 = \Delta T_{max}/5.0/(E^2 \Lambda_b c_b) \tag{25}$$

Since the production rate is proportional to $d_c^2 E$, it will be inversely proportional to E and therefore increase with $t_R^{1/2}$ when the maximum voltage is applied:

$$T_{i,thm} = E \cdot E^{-2} \approx const. \cdot E^{-1} \approx const. \, t_R^{1/2} \tag{26}$$

Summarizing, it is, irrespective of the conductivity of the buffer, always better to work at low electric fields and long run times, which allows large diameters, such that the larger d_c^2 more than compensates the smaller E.

A strategy blindly following this conclusion, however, could lead into the range where the non-uniformity H-contribution predominates dispersion.

Case II. Non-uniformity plate height contribution becomes dominant.

The expression for the plate height with non-uniform migration velocity caused by radial temperature differences within the solutions has been derived by several authors [17–19,29], and can be written as

$$H_{nu} = \frac{1}{384} \frac{d_c^2 \, \Delta u_i^2}{D_i \; u_i} \tag{27}$$

where D_i is the diffusion coefficient of i, and Δu_i is difference in migration velocity over the parabolic profile between centre and wall region. The latter quantity is equal to:

$$\Delta u_i = \delta_i \cdot \Delta T_{lum} \cdot \mu_i E$$
$$= \delta_i d_c^2 \Lambda_b c_b E^3 \mu_i / (16 k_s) \tag{28}$$

where δ_i is the relative change in mobility per degree Kelvin. Substitution leads to

$$H_{nu} = \frac{1}{98\,304} \cdot \frac{\delta_i^2}{D_i} \frac{(\Lambda_b c_b)^2}{k_s^2} \cdot \mu_i \cdot d_c^6 \cdot E^5 \tag{29}$$

The total plate height equals:

$$H_{tot} = 2D_i / u_i + H_{nu} = 2D_i / (E\mu_i) + H_{nu} \tag{30}$$

The requirement to have N plates necessitates a length equal to $N \cdot H$. The length is also tied up to the field strength and the total voltage across the tube: $\Delta V = L \cdot E$. The voltage may be a limiting factor; 20 000 V is as taken as an (arbitrary) practical upper limit. The result, $N \cdot H = \Delta V / E$, leads with Eqs. 32 and 33 to an expression that can be solved for d_c. When the peak-height contribution of the axial diffusion is included, the maximum value of d_c^2 can be expressed as:

$$d_c^2 = \left(\frac{\Delta V}{N_{req}} - \frac{2 D_i}{\mu_i} \right)^{1/3} \left(\frac{98\,304 \; D_i \; k_s^2}{\delta_i^2 \; \Lambda_b^2 \; c_b^2 \; \mu_i} \right)^{1/3} / E^2 \tag{31}$$

When the required plate number is not close to the limiting value, the $2D_i/\mu_i$ term in Eq. 31 is negligible.

Surprising in Eq. 31 is that the allowable diameter is simply inversely proportional to the applied electric field. The first factor at the right

hand side of Eq. 34 reflects the concept of the 'ultimate plate number', given for CZE by $\Delta V \cdot \mu_i / (2D_i)$, as discussed by Knox [16] and Kenndler and Schwer [30]. When the required N approaches this number, the difference given approaches zero; there is no 'room' for allowing any non-uniformity H-contribution and the diameter must go to zero (it does so slowly, though, because of the 1/6 exponent). When the difference becomes negative, the separation is impossible.

The production rate T_i, being proportional to $d_c^2 c_b E$, is in this case inversely proportional to the field strength E and therefore increasing with $t_R^{1/2}$. However, Eq. 31 shows that now T_i increases with $c_b^{1/3}$. When the average temperature increase of the solution was the limiting factor (Case I), the buffer conductivity could be traded in for the capillary cross-section without consequences for the production rate. In the case that the zone broadening by temperature differences in the solution is the limiting factor (Case II), the production rate can be increased by using more concentrated buffers in narrower capillaries. The gain in T_i is not strong, going up with $c_b^{1/3}$ only.

It must be noted, as has been done before by Knox and Grant [16] and Ermakov and Righetti [20], that this contribution to H is usually not of large significance: before it could really become important, the buffer often boils.

Case III. Siphoning contribution to the plate height becomes dominant.

The above expressions point to the use of longer run times and lower fields, which permits to use larger capillary diameters, with an improvement in production rate in proportion to the square root of t_R. Some other limitations then come in sight. One could be the development of gravity-induced natural convection due to density differences in the thermally non-uniform liquid, a phenomenon that plagued electrophoretic experiments in free solution in the early days [31]. Before this happens, however, the longitudinal siphoning flow in the tube resulting from the unavoidable hydrostatic pressure imbalance may spoil the separation. In the following

we will assume that 1 mm 'water head' ($\Delta P = 10$ Pa) pressure difference will be unavoidable.

The mean solvent velocity induced by siphoning, v_{sip}, follows from the Poisson equation:

$$v_{sip} = \frac{d_c^2 \Delta P}{32 \eta L} \qquad (32)$$

The parabolic velocity profile, superimposed on the regular electrophoretic migration, will again lead to an Aris–Taylor-type dispersion effect. Following a similar reasoning as used in Refs. [17,18,29], we find for the plate height contribution by siphoning:

$$H_{sip} = \frac{d_c^6 \Delta P^2}{98\,304 \eta^2 L^2 D_i E \mu_i} \qquad (33)$$

In a way similar to what we have done in Case II a maximum capillary diameter can be found:

$$d_c = \left(\frac{1}{N_{req}} - \frac{2D_i}{\Delta V \mu_i} \right)^{1/6} \left(\frac{98\,304 \eta^2 \Delta V^3 D_i \mu_i}{\Delta P^2 E^2} \right)^{1/6} \qquad (34)$$

As in Eq. 31, the diffusion term $2D_i/(\Delta V \mu_i)$ in the right-hand side of Eq. 34 often can be neglected.

The equation shows that the allowable diameter is proportional to $E^{-1/3}$. The production rate T_i, being proportional to $E d_c^2$, goes up with $E^{1/3}$, quite contrary to what happens in Cases I and II, where a beneficial effect of a low electric field was predicted. Since siphoning does not depend on the conductivity κ of the solution, in this case the production rate simply increases with c_b.

Combination of three limitations
Circular capillaries

Depending on the conditions, one, two or in exceptional cases all three of the limitations are in effect. As each limitation in the above sections was expressed in terms of the maximum value of d_c compatible with the preset requirements on t_R and N, the limitation leading to the smallest d_c value determines the ultimate production rate.

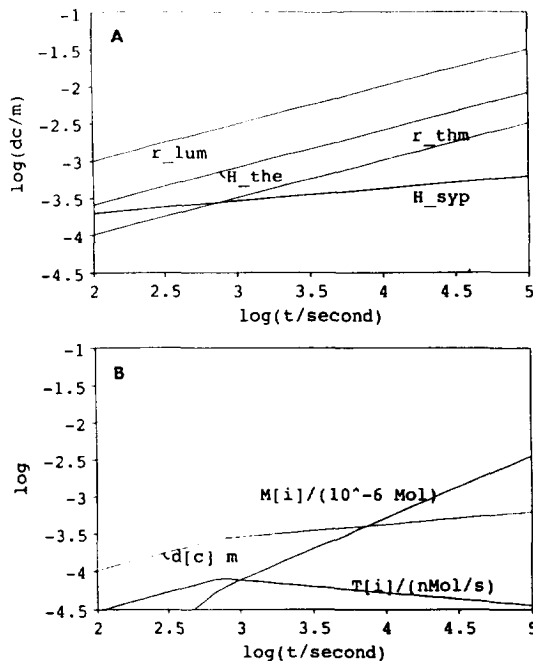In Figs. 1 and 2 we have plotted the maximum diameters, according to Eqs. 25, 31 and 34,

Fig. 1. (A) Maximum diameters for a circular capillary (log $d_c/$m), according to Eqs. 25, 31 and 34. Conditions: required plate number $N = 200\,000$. $\Delta V = 20$ kV, $c_b = 0.003$, $\beta_{EMD,i} = 0.1$, $\Delta P = 10$ Pa and $\Delta T_{max} = 10$ K, $\mu_i = 30 \cdot 10^{-9}$ m^2 s^{-1} V^{-1}, $D_i = 10^{-9}$ m^2/s, $\eta = 10^{-3}$ kg m^{-1} s^{-1}, $\delta_i = 0.023$, $r_{thm} = 5.0$ K/(W/m). Line indicators: 'r_lum': maximum diameter to keep ΔT in lumen below 10 K; 'H_the': maximum diameter to keep plate height due to thermal non-uniformity sufficiently low to obtain required plate number (Eq. 34); 'r_thm': maximum diameter to keep ΔT in air bath below 10 K; 'H_syp': maximum diameter to keep plate height due to siphoning sufficiently low to obtain required plate number (Eq. 37). (B) Production rate T_i {plotted as log[$T_i/$(nmol/s)]}, amount in single run, M_i, (plotted as log M_i/μmol) and maximum diameter d_c [plotted as log($d_c/$m)] as a function of run time.

found for conditions and requirements that appeared appropriate: $\Delta V = 20$ kV, $c_b = 0.003$, $\beta_{EMD,i} = 0.1$, $\Delta P = 10$ Pa and $\Delta T_{max} = 10$ K, with (overall) mobility of $\mu_i = 30 \cdot 10^{-9}$ m^2 s^{-1} V^{-1}.

The diffusion coefficient D_i was taken as 10^{-9} m^2/s, and the viscosity as 10^{-3} kg m^{-1} s^{-1}, while δ_i was assumed to be 0.023.

Fig. 1 applies to the case when $N = 200\,000$ plates are required, close to the theoretical limit of 300 000 for $\Delta V = 20\,000$ V. In Fig. 1A it is seen that the two limitations of importance are those
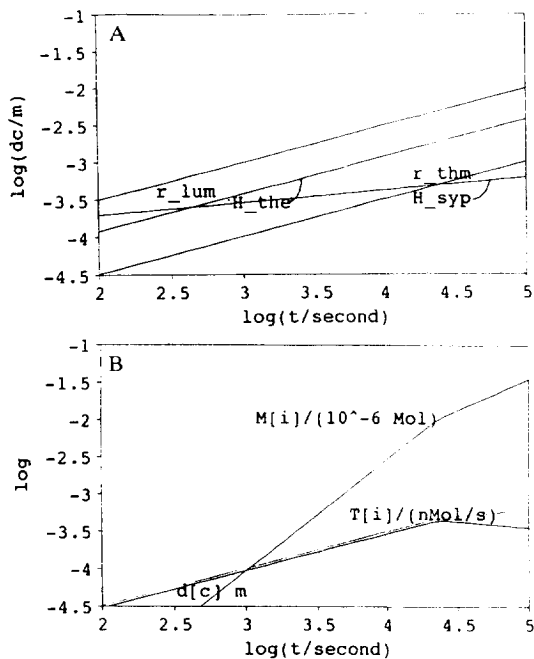
Fig. 2. (A) Maximum diameters, for a circular capillary, according to Eqs. 25, 31 and 34. Conditions: $c_b = 0.03$. Other conditions as in Fig. 1. (B) As in Fig. 1.

of the absolute temperature increase ('r_thm'), set here at 10 K, and the siphoning effect ('H_sip'). The first limitation is important at fast runs at high field, forcing the use of small diameters, the second being important at long run times and weak fields, with corresponding increase in admissible diameters. The 'break-even' point lies at $t_R = 800$, corresponding to a field E of 30 000 V/m, with a diameter d_c of 280 μm and a tube length of 0.7 m.

As explained above, when accepting longer run times, one enters the range of the siphoning limitation. The admissible diameter goes up with t_R only slowly, not fast enough to compensate for the slower operation of the system. As can be seen in Fig. 1B, from the break-even point on the production rate goes down, although the production per run keeps increasing at a slower pace. In this realm it is better to repeat faster runs, rather then to try to devise an experiment where the required material can be collected in one run.

It is important to be aware of the strong

dependence of these relations on the parameters chosen for the calculations. The most important one is probably the c_b value, for which a rather low value was chosen here (0.003 mol/l). A ten times higher value would move down the 'r_thm'-line in Fig. 1A over half a log unit. When the choice would have been to work at the lower end of the t_R scale, left of the 'break-even' point (rather close to common CE-conditions), the net effect would be zero: Although the diameter goes down, this is exactly compensated by the larger concentration loadability of the more concentrated buffer.

However, the 'H_sip' line would stay in the same position. The 'break-even' point therefore would move to higher t_i values. This is shown in Fig. 2 where a ten times higher buffer concentration was chosen than in Fig 1. A higher maximum production rate is found when the time required for a simple run is not limited and the optimum value of the capillary length can be used, the production rate increases with $c_b^{3/4}$. The final limit of the production rate in this case will be set by changes of the selectivities found in high-ionic strength solutions or by the limited solubility of the buffer or the analyte.

Another parameter with a strong influence is $\beta_{EMD,i}$. The assumed value, 0.1, is about the best one can expect under carefully tuned buffering conditions. Since the production rate is directly proportional to its inverse, the absolute values of T_i and M_i, as given in the figures, can turn out to be much smaller in practical situations, e.g., where the buffer choice has not been carried out with extreme care, or when it is simply impossible to tune the buffer to the requirements in various critical parts of the electropherogram.

In Fig. 3 the results are shown when a lower value (50 000) for the required plate number is assumed. Compared to Fig. 1, the lines representing the limitations on d_c have moved up, that for the temperature increase more strongly than that for the siphoning effect. As a result, the 'break-even' point has moved to the right. The maximum production rate is increased with a factor of approximately seven, obtained at an optimal run time for a single run, which is approximately three times longer. This increase
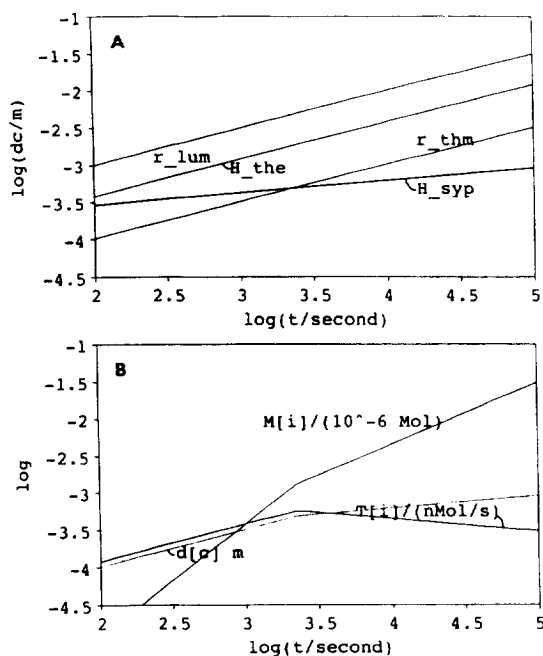
Fig. 3. (A) Maximum diameters, for a circular capillary, according to Eqs. 25, 31 and 34. Conditions: required plate number $N = 50\,000$. Other conditions as in Fig. 1. (B) As in Fig. 1.

of T_i with the looser demands on the separation sharpness can be explained by two factors. First, the maximum concentration of the analyte as well as the peak volume are increased, both proportional with $N^{-1/2}$, as has been shown in previous sections. This gives already a factor of four in the production rate going from 200 000 to 50 000 for N_{req}. The second factor is the shift of the maximum towards the more advantageous low fields and long run times. This generally gives an extra gain proportional to $N^{-1/4}$. In this particular example the gain is even larger because with $N_{req} = 200\,000$ the allowed plate height is partially already consumed by the axial diffusion term.

Rectangular ducts.

The cylindrical configuration is experimentally convenient. However, from the point of view of heat conduction it is the worst configuration possible. For all of the three main resistances to heat transfer, i.e., in the lumen (lum), the wall

and the thermostatting medium (thm), the Nusselt number is larger [28] for flat rectangular ducts having the same cross-sectional area. Thus, all of the above conclusions apply equally well to such a design, with suitable adjustment of the constants.

The thermal effects and dispersion in so-called rectangular (rather ellipsoidal) fused-silica capillaries have been studied theoretically [32–34], as well as experimentally [27,35]. In such a channel, with dimensions $2a$ by $2b$, with $a < b$ and $\phi = b/a$, the thermal effect ('r_lum') and the dispersion connected with it ('H_the') are controlled [32–34] mainly by the height of the channel, i.e. $2a$. This provides an important feature of the rectangular columns compared to the circular tubing, since by increasing the width, b, of the rectangular capillary while keeping the height, a, constant, the sample capacity is improved without affecting the efficiency due to thermal effects. Moreover, by keeping the same height, a, the heat dissipation remains constant, which allows to maintain the same separation voltage, without loosing analysis speed.

In Fig. 4 the mean temperature rise in the lumen for a circular and a rectangular column against the electric field is shown. The temperature rise was calculated from the variation between the experimental electric current and the
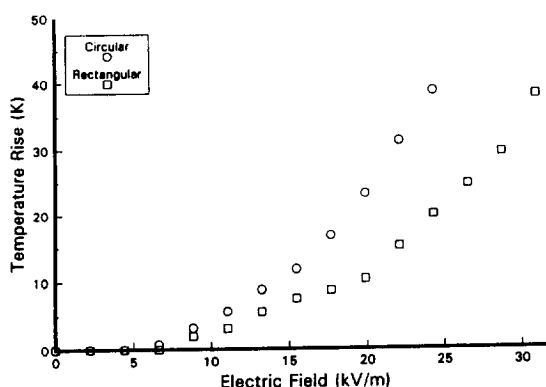

Fig. 4. Temperature rise against the electric field for a circular and a rectangular capillary (modified from Ref. [25]). Conditions: 0.05 M 3-(cyclohexylamino)-1-propanesulfonic acid (CAPS) buffer, pH 10.4. Capillaries: circular 200 μm I.D. and rectangular 500×50 μm, both with the same total length (90.5 cm).

hypothetical one that would be obtained if no thermal effects were present, and assuming that a 2% variation in the electric current is equivalent to a temperature rise of 1 K. Results show that the temperature rise is larger in the circular capillary than in the rectangular one. This is partly due to the larger cross-sectional area of the circular column (25% larger). However, at higher voltages the difference in current is much larger than 25%. Also, Fig. 4 demonstrates that for the same temperature rise the rectangular capillary allows a higher run voltage. Moreover, the higher the voltage applied, the larger the difference between both capillaries.

In view of these promising experimental results, we found it attractive to repeat the exercises documented in Fig. 1 for parameter values that appear to apply to such rectangular ducts. We assumed rectangular cross-sections (although they were in reality not quite so) and applied the numerical values found in Ref. [34] for the non-uniformity dispersion, the pressure-induced flow and the dissipation-induced temperature rise in the lumen. Equations equivalent to Eqs. 25, 31 and 34 allowed us to calculate the effects denoted by 'r_lum', 'H_the' and 'H_sip' for such channels.

For the air-bath temperature drop, 'r_thm', we had to make a similar wild guess as we were forced to make in the case of circular tubes. Based on our own results, we decided to use $r_{thm} = 5.0$ K/(W/m), equal to the value assumed for circular ones. It is likely that the value in fact could be lower, but this choice has the additional advantage that there is no ill-justified bias towards the rectangular geometry.

The results are shown in Figs. 5 and 6. For d_c we used 'equivalent' values, i.e. d_c is the diameter of a circular tube having the same cross-sectional area. In Fig. 5 the width-to-height ratio was 10, close to the value estimated for the ellipsoidal capillaries (50×500 μm) used in some of our earlier experiments [28].

Comparison of this figure with Fig. 1 in the first place shows that the limiting factors 'r_thm' and 'H_sip' are the same. With the choice of r_{thm} being equal, the 'r_thm' branches in the plots are identical; for the outside dissipation the geome-

Fig. 5. (A) Maximum equivalent diameters, $d_c = \sqrt{4/\pi \ \text{area}}$, for a rectangular capillary, according to Eqs. 25, 31 and 34. Conditions: required plate number $N = 200\,000$. Width to height ratio of rectangular channel $\phi = 10$. Other conditions as in Fig. 1. (B) As in Fig. 1.

try of the inner channel is not important. Thus, on the left side all the plots are identical. The 'H_the' plot lies at higher values for the rectangular tubes (as elaborately discussed in Ref. [34]), but that is irrelevant since this effect never sets a limit to the production rate.

The difference between Fig. 5 on the one hand and Fig. 1 on the other resides in the smaller influence of the siphoning effect. The low flow permeability of the flattened channel, leading to small velocities at the head pressure of 10 Pa, allows to go to larger areas (equivalent d_c) without serious deterioration of the efficiency. For instance, in Fig. 5A it can be seen than the 'break-even' point between 'r_thm' and 'H_sip' is at about $t_R = 6000$ s, with 'd_c' = 700 μm, while for a circular capillary the values are $t_R = 800$ s and $d_c = 250$ μm. An improvement of about a factor of three in the production rate T_i is the result. It should be noted that 'd_c' here is an
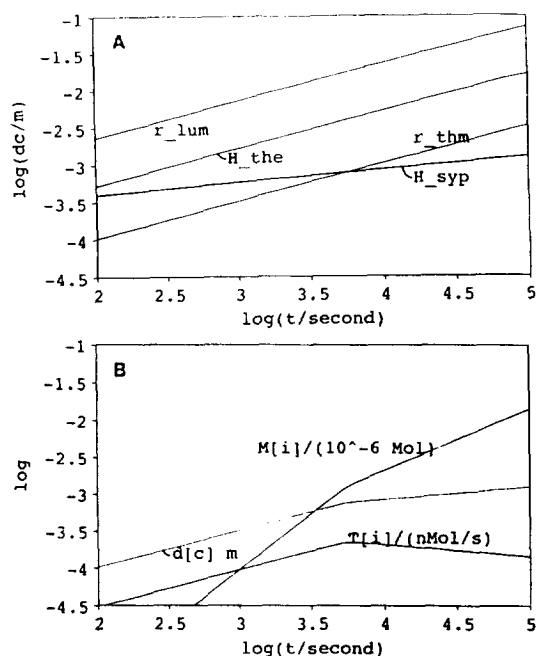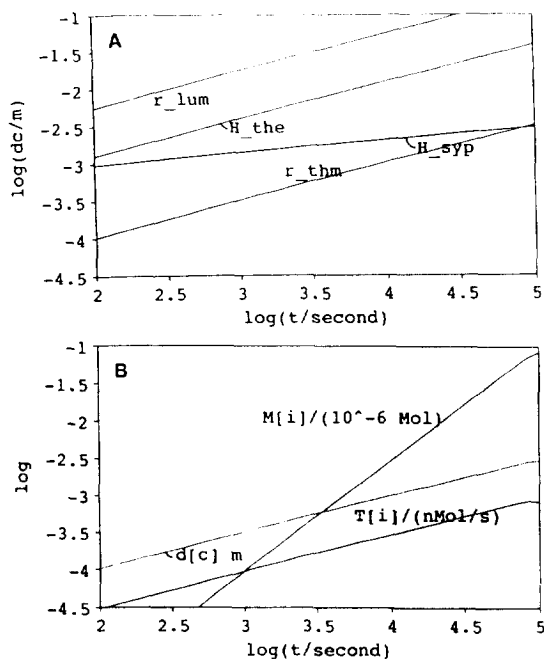
Fig. 6. (A) Maximum equivalent diameters, $d_c = \sqrt{4/\pi}$ area, for a rectangular capillary, according to Eqs. 25, 31 and 34. Conditions: required plate number $N = 200\,000$. Width to height ratio of rectangular channel $\phi = 64$. Other conditions as in Fig. 1. (B) As in Fig. 1.

'equivalent' value; 700 μm corresponds for $\phi = 10$ to dimensions of about 200×2000 μm.

In Fig. 6 it is shown that a further increase of the production rate can be obtained when rectangular capillaries with $\phi = 64$ were available. However, the predicted optimum in T_i lies rather far away from contemporary CE conditions, with a run time of 80 000 s and a capillary height and width of 340 and 22 000 μm. It is doubtful whether the extrapolation of our insights in CE behaviour to such dimensions is justified. Certainly, experimental work would be needed to verify this.

3. Conclusions

This work was undertaken in order to derive general guidelines for optimization of CE, under the constraint of a fixed required plate number.

when production per time unit is important. It is therefore appropriate to summarize the conclusions, and to indicate further research directions. The most important aspect is the choice of the background electrolyte (BGE). With acid–base-type sample constituents (the majority of the cases), manipulation of the pH can lead to the best 'selectivity' (ratio of mobilities), for which the required plate number is as low as possible. Production rate is directly proportional to $1/N$. When the pH has been decided upon, it may be worthwhile to investigate various buffer systems with this pH value, in order keep the electromigration dispersion (EMD) as low as possible. A low EMD allows the use of high concentration loads. Analytical expressions as well as numerical procedures are available to predict EMD. The optimization of the geometry amounts to increasing the diameter as far as possible. At low accepted run times, using short tubes, this is limited by the absolute temperature rise in the lumen. Accepting longer run times it is possible to increase the diameter, and to improve the production rate, roughly by a factor of $\sqrt{10}$ for a ten times longer run time. This approach finds, as far as we can see, its end when the siphoning in wider tubes affects the efficiency significantly. The point where this happens is in the range of practical CE conditions for high plate numbers and low buffer concentrations. For small plate numbers and higher buffer concentrations the points lies outside the range where predictions about CE conditions are believed to be reliable.

Keeping within the realistic range, the theoretical results for a preparative CE system can be compared with those obtained in a typical analytical-scale CE system. As has been pointed out in the introduction, in an analytical system with a 0.03 mol/l buffer concentration, typically $8 \cdot 10^{-12}$ mol of analyte can be purified in 10 min, giving a production rate of approximately 10^{-14} mol/s. With the same buffer concentration in Fig. 2B a maximum production rate of $5 \cdot 10^{-13}$ is predicted, a factor of 50 higher than for the analytical system. The time for a single run to obtain this result is approximately 6 h.

Rectangular or ellipsoidal shaped capillaries have important promises for the increase of

sample capacity and production rate. The main reason is that the smaller flow permeability (for the same area) allows to increase the area without development of pressure-induced flow. If conditions can be found where external heat transfer is also better in these capillaries, the prospects would be even better.

References

[1] J.W. Jorgenson and K.D.A. Lukacs, Anal. Chem., 53 (1981) 1298–1302.
[2] R.P.W. Scott and P. Kucera, J. Chromatogr. Sci., 12 (1974) 473–485.
[3] A. Guttman, A.S. Cohen, D.N. Heiger and B.L. Karger, Anal. Chem., 62 (1990) 137–141.
[4] D.J. Rose and J.W. Jorgenson, J. Chromatogr., 438 (1988) 23–29.
[5] C. Schwer and F. Lottspeich, J. Chromatogr., 623 (1992) 345–355.
[6] K.D. Altria and Y.K. Dave, J. Chromatogr., 633 (1993) 221–225.
[7] A.W.J. de Jong, H. Poppe and J.C. Kraak, J. Chromatogr., 148 (1978) 127–141.
[8] F.E.P. Mikkers, F.M. Everaerts and Th.P.E.M. Verheggen, J. Chromatogr., 169 (1979) 1–10.
[9] F. Foret, S.F. Ossicini and P. Bocek, J. Chromatogr., 470 (1989) 299–308.
[10] J.L. Beckers, J. Chromatogr. A, 693 (1995) 347.
[11] H. Poppe, Anal. Chem., 64 (1992) 1908–1919.
[12] X. Xu, W.T. Kok and H. Poppe, in preparation.
[13] S.V. Ermakov, M.Y. Zhukov, L. Capelli and P.G. Righetti, Anal. Chem., 66 (1994) 4034.
[14] F. Helfferich and G. Klein, Multicomponent Chromatography, Marcel Dekker, New York, 1970.
[15] F.E.P. Mikkers, F.M. Everaerts and Th.P.E.M. Verheggen, J. Chromatogr., 169 (1979) 11–20.
[16] J.H. Knox, Chromatographia, 26 (1988) 329–337.
[17] R. Virtanen, Acta Polytech. Scand., 123 (1974) 1–67.
[18] J.H. Knox and I.H. Grant, Chromatographia, 24 (1987) 135–143.
[19] E. Grushka, R.M. McCormick and J.J. Kirkland, Anal. Chem., 61 (1989) 241–246.
[20] S.V. Ermakov and P.G. Righetti, J. Chromatogr. A, 667 (1994) 257.
[21] G.J.M. Bruin, P.P.H. Tock, J.C. Kraak and H. Poppe, J. Chromatogr., 517 (1990) 557–572.
[22] R.J. Nielsen, A. Paulus, A.S. Cohen, A. Guttman and B.L. Karger, J. Chromatogr., 480 (1989) 111–127.
[23] R.H. Perry and C.H. Chilton, Chemical Engineers' Handbook, McGraw-Hill, Tokyo, 1973.
[24] S.T. Hsu, Engineering Heat Transfer, Van Nostrand, New York, 1963.
[25] J.H. Knox and K.A. McCormack, Chromatographia, 38 (1994) 215–221.
[26] R. Hilpert, Forsch. Gebiete Ingernieurw., 4 (1933) 215.
[27] J.K. Towns and F.E. Regnier, Anal. Chem., 64 (1992) 2473–2478.
[28] A. Cifuentes and H. Poppe, Electrophoresis, in press.
[29] G.D. Roberts, P.H. Rhodes and R.S. Snyder, J. Chromatogr., 480 (1989) 35.
[30] E. Kenndler and C. Schwer, Anal. Chem., 63 (1991) 2499–2502.
[31] S. Hjertén, Chromatogr. Rev., 9 (1967) 122–219.
[32] R. Aris, Proc. Roy. Soc. A, 252 (1959) 538–550.
[33] M.J.E. Golay, J. Chromatogr., 216 (1981) 1–8.
[34] A. Cifuentes and H. Poppe, Chromatographia, 39 (1994) 391–404.
[35] Z. Ryšlavy, P. Bocek, M. Deml and J. Janák, J. Chromatogr., 144 (1977) 17.